



Modeling and Assessment of Power Consumption for Green Machining Strategy

Jung-Jae Won¹ · Yong Ju Lee^{1,2} · Yu-Jin Hur¹ · Sang Won Kim³ · Hae-Sung Yoon^{1,2}

Received: 29 October 2021 / Revised: 29 April 2022 / Accepted: 20 July 2022 / Published online: 25 August 2022
© The Author(s), under exclusive licence to Korean Society for Precision Engineering 2022

Abstract

Energy-saving technologies seek to minimize the environmental burden caused by manufacturing. In this study, it is aimed to develop a sustainable machining strategy that reduces the energy consumed during metal cutting, via modeling and assessment of power consumption of the process. Three perspectives, smart, optimal, and universal, are used to review the literature and define the strategic requirements. Based on the perspectives, the power consumption data was utilized to monitor the process in real-time and to control the process to be sustainable with a wide variety of cutting conditions and manufacturing environments. A power-prediction model was constructed, and two adaptive feed-control schemes were suggested. One controls the feed, while the other controls the feed per tooth. The experimental results show that both control schemes were up to 18% energy efficient with the given geometries and easily applicable over a wide range of conditions and satisfied the requirements set out above. The efficiencies of the control methods were discussed with respect to the control criteria, constraints, and materials. It is expected that this research will facilitate sustainable machining.

Keywords Energy-saving · Time-saving · Specific energy consumption · Material removal rate · Machining strategy

Abbreviations

a_e	Radial depth of cut (mm)
a_p	Axial depth of cut (mm)
D	Diameter of cutting tool (mm)
F	Feed (mm min ⁻¹)
f_z	Feed per tooth (mm flute ⁻¹)
MRR	Material removal rate (mm ³ s ⁻¹)
N	Rotational speed of the spindle (rpm)
$P_{cutting}$	Power consumed in material removal (W)
$P_{machine}$	Power consumed by a machine when the material is not removed (W)
P_{total}	The total power consumed during cutting (W)

SEC	Specific energy consumption (J mm ⁻³)
V_c	Cutting speed (m min ⁻¹)

1 Introduction

Eco-friendly manufacturing attracts considerable attention in the present era of global warming. Many researchers have investigated the energy consumption during metal cutting, which is a core feature of many manufacturing sectors [1]. Various technologies have been developed for the sustainable and environmentally benign process, in the area of process improvements, high-efficiency machine tools and components, and process optimization. [2]

For process improvements, cutting-tool lubrication and cooling have been widely investigated; these directly affect machinability and tool wear [3]. Minimum quantity lubrication (MQL) has been employed to control the coolant supply using an optimal injection pressure; [4, 5] this reduces energy consumption. Replacement of cutting oil by a nanofluid [6, 7] has been combined with MQL or cryogenic machining, to increase productivity and process stability. Modification of tool geometry [8] and tool-surface coatings [9] improve efficiency and increase tool life. High-pressure

✉ Hae-Sung Yoon
hsyoon7@kau.ac.kr

¹ School of Aerospace and Mechanical Engineering, Korea Aerospace University, 76 Hanggongdaehak-ro, Deogyang-gu, Goyang-si, Gyeonggi-do 10540, Republic of Korea

² Department of Smart Air Mobility, Korea Aerospace University, 76 Hanggongdaehak-ro, Deogyang-gu, Goyang-si, Gyeonggi-do 10540, Republic of Korea

³ Duckheung Co., Ltd., 26, Bonsan-ro 110 beon-gil, Jinyeong-eup, Gimhae-si, Gyeongsangnam-do 50857, Republic of Korea

pumps and sensors are used to control coolant flow, [10, 11] enhancing pumping efficiency.

Otherwise, energy consumption during metal cutting is significantly influenced by the machine tool per se. Drake et al. [12] used a six-step method to measure the energy consumptions of the various sub-components of machine tools. Eighty percent of the total energy consumed was by machine control, spindle rotation, and coolant pump operation, not by material removal. High-efficiency machine tool components contribute markedly to energy-saving. Yoon et al. [13] measured the feed drive power consumptions of various machine tools during multi-axis movements. The power-consumption characteristics varied greatly by the machine, and energy-saving strategies must thus differ when encountering various machine-tool configurations.

For process optimization, adaptive feed control (AFC) has been widely used to conserve energy by distributing cutting loads and reducing the cycle time with the adjustment of cutting conditions. AFC adjusts the cutting conditions via real-time monitoring of process indicators (for example, the cutting force or the spindle load). Yazar et al. [14] implemented a feed-control strategy by applying a cutting force model to a three-axis milling machine. The feed rate was increased when the cutting force was below the reference value and was reduced at higher values. Energy consumption was reduced by minimizing the cycle time. Similarly, the spindle load has been used to control the feed [15, 16]. AFC is currently offered by many machine-tool manufacturers, including Heidenhain and Siemens and has been applied to commercial solutions. Feed optimization is simple and markedly reduces energy consumption [17–19]. Therefore, in this study, based on the conventional AFC, it was attempted to establish an improved energy-saving strategy from various perspectives.

In this research, three perspectives were suggested, particularly to discuss the future of sustainable processes based on a review of existing technologies. First, a “smart” strategy that can be directly, automatically, and precisely applied is required. “Smart” strategy has been extensively investigated for economical and energy efficient processes as well as environmental benefits [20]. However, some conventional techniques are not simple; complex calculations are required in most cases. If AFC employs the cutting forces, such forces must be measured by (expensive) sensors or calculated using a model [21, 22]. This control method thus utilizes calculated values, not those obtained by monitoring in real-time. In practical cases, it is also extremely difficult to calculate the current cutting force in real-time, particularly during of complex shapes. Some commercial solutions use the real-time spindle load to control the process. However, the load is calculated based on the spindle input current; neither the precision nor the response time may be optimal. It is thus required

to develop a strategy dealing with real-time parameters with simpler calculations and shorter response time than cutting forces or spindle current.

Second, a strategy that defines an “optimal” direction is essential when dealing with a wide variety of process parameters. Conventional technologies usually employ one-on-one substitution of optimal parameters depending on the cutting conditions experienced by a specified tool. However, prior calculations or preliminary experiments that cover all possible cutting conditions are impossible in a real-world factory. Thus, both well-verified data obtained over a certain range, and an optimization algorithm that handles arbitrary process changes are required; the efficiency of any strategy must be ensured as process conditions vary.

Third, a “universal” strategy is required to handle the wide variety of manufacturing environments. Some conventional technologies require specific hardware or software, and their efficiency is thus limited in terms of material and the processing range. For example, if high-efficiency pumping or MQL is required, existing equipment must be replaced. Also, if the work material changes, it is not easy to predict the strategic efficiencies. Thus, any effective technology should be widely applicable.

Therefore, this research aims to ensure “smart, optimal, and universal” themes in AFC to save energy during milling. Here, the power consumption of the machine tool, which is a real-time parameter, was utilized to control the process to be sustainable with simple calculations. Based on the themes mentioned above, schemes of two different control methods were suggested and verified experimentally to confirm their utility. By adjusting one or two cutting parameters, both methods effectively distributed the cutting loads to reduce the cycle time and total energy consumption. The results were discussed to develop a “smart, optimal, and universal” strategy. From the power data, material removal rates (MRRs) were estimated. This simplifies optimization; given the machine data and basic material information, the MRR was derived without the need to calculate physical cutting loads or to consider cutting geometries, and without any pre-or post-processing.

The energy reductions afforded by varying process parameters and work materials were discussed in the context of the relationship between specific energy consumption (SEC) and the MRR. This enables optimization of process parameters and calculation of energy reductions under all conditions. Also, this study dealt with a titanium alloy, a representative difficult-to-cut material with several cutting constraints. The experimental results were analyzed and compared to literature data on the machining of other materials. The efficiencies of the new methods were discussed from the perspective of material properties. It is expected that results from this study will simplify the milling of many engineering materials.

2 Experimental Details and Control Methods

To evaluate control methods, a three-axis machining center (Robodrill α -k10c; Fanuc Corp., Japan) equipped with a turret for an automatic tool changer (ATC) was used. A four-flute plain-end mill of diameter 12 mm (SED-4120U-TTT5515; Taegutec Ltd., Korea), specifically designed to cut titanium alloys, was employed. Power data (in W) were collected by a power meter (PAC4200, Siemens, Germany) running customized Labview software. The sampling frequency was 10 Hz. The power meter used for data collection was installed on the switchboard of the machining center; it thus did not affect processing at all. The base material was Ti-6Al-4 V (ASTM B265 Grade 5; Sejin Titanium, Korea). The experimental setup and tool are shown in Fig. 1.

2.1 The Power Consumption Model

Initially, power consumption experiments were performed to construct an empirical model relevant over a given range. A full empirical model is not necessary for control methods, but is here used to yield comprehensive and precise estimations. Basically, the experiments extended the model range of a preceding study [23]. The spindle rotation speed, feed rate, and the axial and radial depth of cut are the principal factors that affect power consumption; all were divided into three levels. There were thus 81 cutting conditions, but 27 conditions were evaluated with a 1/3 partial experiment on this study. All experiments were repeated three times per each condition.

Table 1 shows the cutting conditions by the factors studied, where a_p is the axial depth of cut and a_e is the radial depth of cut. An overview of single-slot cutting is shown in Fig. 2a. First, the cutting position was attained rapidly. The desired a_p was set in the $-Z$ direction and a 40-mm-cut was created in the $+X$ direction. The tool was exited via movement in the $+Z$ direction, and the next slot was then rapidly attained.

Power consumption was analyzed based on the power profile and divided into the subcomponents $P_{machine}$ and $P_{cutting}$ following literature [24]. For example, the profile at 1,500 rpm rotation, 200 mm min^{-1} feed, an a_p of 4 mm, and an a_e of 12 mm is shown in Fig. 2(b). $P_{machine}$ (about 600 W) is the mechanical power consumed by the machine when material is not removed. This includes the standby power and the power required for machine movements and the coolant pump. $P_{cutting}$ is the power used to remove material (only). P_{total} is the sum of instantaneous total power consumed during cutting (P_{total} ; the sum of $P_{machine}$ and $P_{cutting}$).

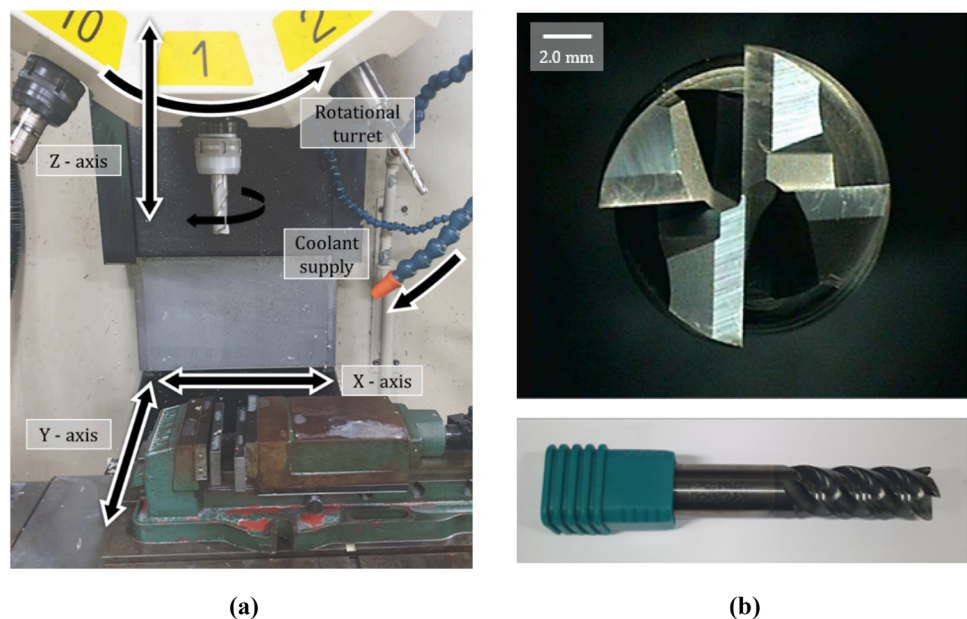
2.2 Schematics of the Control Methods

Figure 3 is an experimental diagram and shows the sequence from machining to control method application. Based on

Table 1 Cutting conditions when evaluating energy consumption

Level	Rotational speed (rpm)	Feed (mm min^{-1})	a_p (mm)	a_e (mm)
-1	1,000	100	2	4
0	1,250	200	3	8
+1	1,500	300	4	12

Fig. 1 The experimental tools. **a** Machine-tool configuration. **b** The cutting tool designed for work with Ti alloys



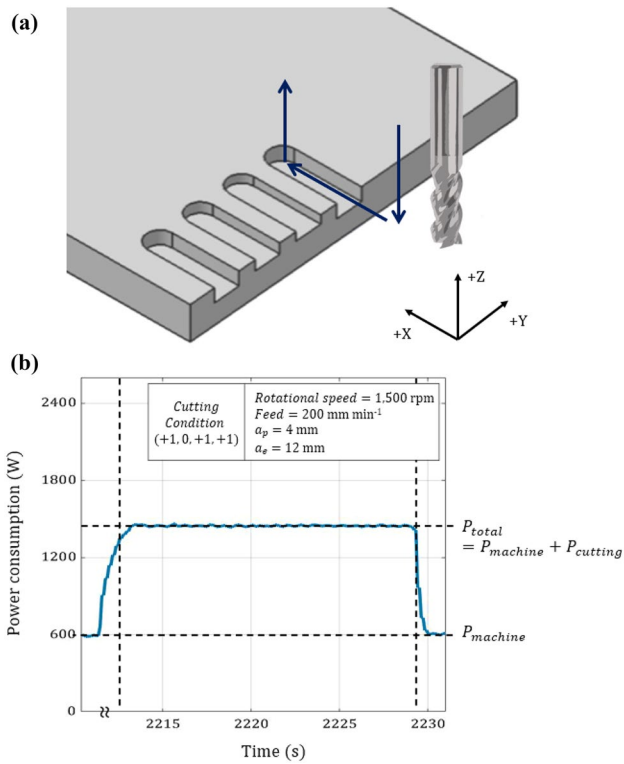


Fig. 2 The model used to predict power consumption during cutting. **a** A schematic of an experiment. **b** The power profile at 1500 rpm rotation, 200 mm min⁻¹ feed, $a_p = 4$ mm, and $a_e = 12$ mm

the constructed model, the power consumed for material removal was calculated. The power consumed for material removal was then utilized to adjust process parameters (one-factor or two-factor). Both control methods were applied to

process two types of workpiece shapes (stepped and wave shapes) and analyzed in terms of energy consumption and processing time. Finally, the energy-saving of the two control methods was evaluated from three perspectives: “*smart, optimal, and universal.*”

Here, the schematics of the control methods were described by reference to the number of control variables. Before implementing a control method, experiments were performed using a schematic to verify the energy-saving effects. Basically, the schemes exploit the linearity between MRR and the cutting power, $P_{cutting}$, as will be proven in the Discussion section. Each control scheme is shown in detail, with the sample geometries used for verification.

Two types of workpiece shapes were explored to verify that the methods afforded energy reductions with instantaneously changing cutting volumes. First, to allow power variations to be observed simply, the workpiece cutting volume was varied in a stepwise manner. Figure 4a shows the shape and specifications of the workpiece geometry, termed a “stepped shape”, below. The cutting tool moved along a fixed line. a_p was held constant at 3 mm, and a_e increased or decreased at regular intervals of 4, 8, or 12 mm. Second, a relatively complex wave geometry, (here termed the “wave shape”) was used. Two arcs of radii 8 and 10 mm intersected at intervals of 120° (Fig. 4b). The cutting consists of two steps; the wave shape was created first by the “curved cutting” as noted in the figure, and then was removed by the “straight cutting”. During the curved cutting, the geometry was divided into 8 Sects. (30° each) (Fig. 4c) and process parameters were controlled independently at each section. Then, a_e was calculated by dividing the area of each section by the movement length of the cutting tool center line. The

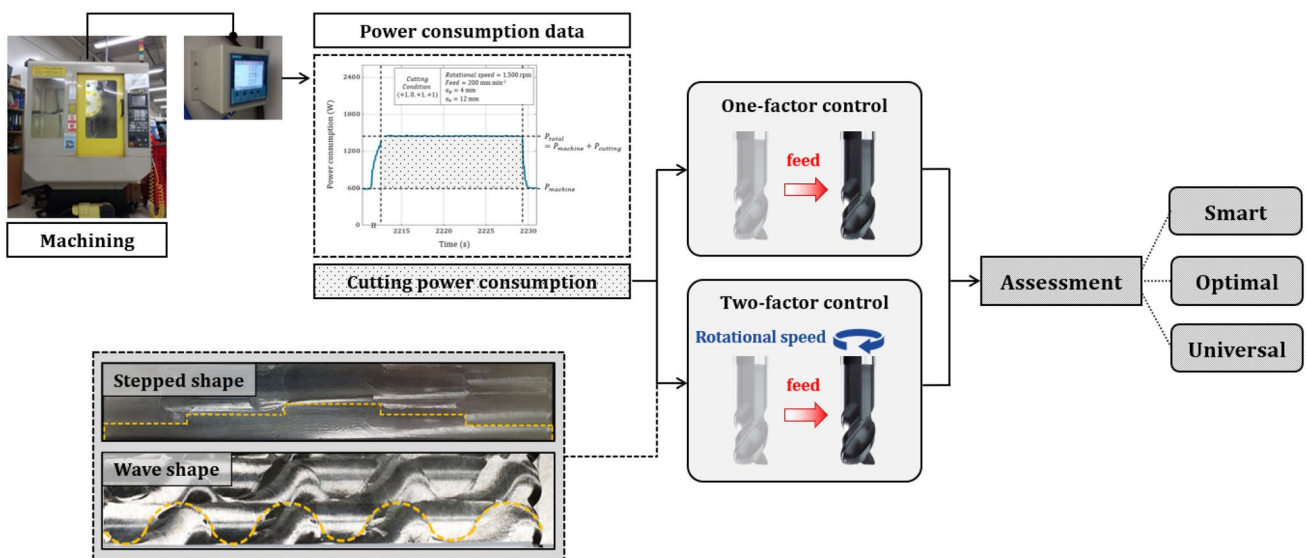
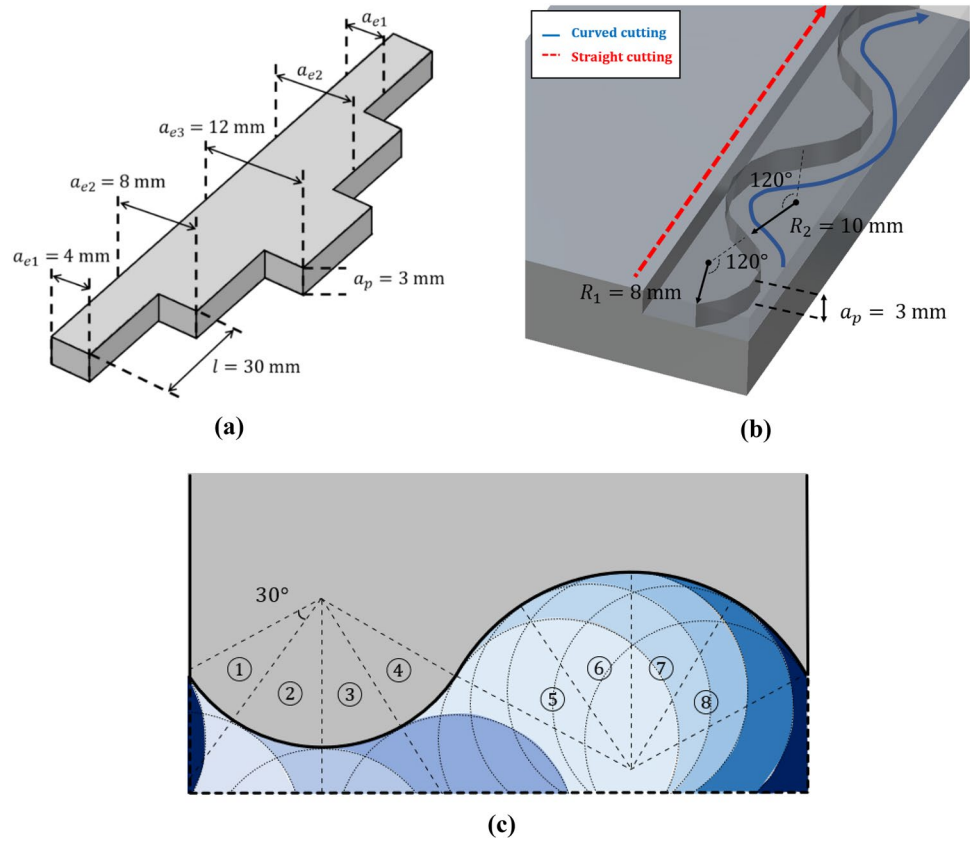


Fig. 3 Experimental diagram

Fig. 4 The cutting models. **a** Stepped shape. **b** Wave shape. **c** Schematic diagram of equalization (8 sections, 30° each)



same control methods were applied to both shapes, and the energy consumptions and cycle times were measured.

2.2.1 One-factor Control Method

The one-factor control method adjusts a single feed factor. Feed-control methods have been widely utilized in AFC strategies [17–19]. However, this method approximates the cutting load by calculating the MRR from the cutting power, $P_{cutting}$, measured by an external power meter, rather than by calculating the cutting force or measuring the spindle load. In practical cases, it is extremely difficult to calculate the current MRR in real-time, particularly during high-speed machining of complex shapes. The cutting power affords easier estimation of the MRR, and faster responses than those of the internal current calculation of machine tools [25]. By equating an increase or decrease in the feed to an

increase or decrease in the MRR, the MRR was maintained, and the total energy consumption and cycle time were measured.

Table 2 shows the cutting conditions for the stepped shape. To verify the control scheme, the process parameters were first based on the MRR, and the results were compared. The spindle rotation speed was set to 1,250 rpm (cutting speed of 47.12 m min^{-1}), within the acceptable speed range (30 to 70 m min^{-1}) of the tool manufacturer. In the “one-factor control group”, the MRR was maintained constant throughout the entire experiment (at $60 \text{ mm}^3 \text{ s}^{-1}$). However, in the “conventional” group, the entire section was cut at a constant feed rate (150 mm min^{-1}) using an intermediate a_e (8 mm) and an MRR of $60 \text{ mm}^3 \text{ s}^{-1}$, thus without MRR-based optimization.

Similar to the stepped shape, the process parameters were controlled for the wave shape. Tables 3 and 4 show the

Table 2 Sample processing conditions (cutting load distributions) for the stepped shape

Radial depth of cut a_e (mm)		4	8	12	8	4
Constants		Spindle rotation speed = 1,250 rpm, $a_p = 3 \text{ mm}$				
Conventional	Feed (mm min^{-1})	150, constant				
	MRR ($\text{mm}^3 \text{ s}^{-1}$)	30	60	90	60	30
One-factor control	Feed (mm min^{-1})	300	150	100	150	300
	MRR ($\text{mm}^3 \text{ s}^{-1}$)	60, constant				

Table 3 Sample processing conditions for the wave shape (curved cutting)

Constants		Spindle rotation speed = 1,250 rpm, $a_p = 3$ mm							
Conventional	a_e (mm)	5.30							
	Feed (mm min ⁻¹)	150, constant							
	MRR (mm ³ s ⁻¹)	39.75 (average value)							
One-factor control	Section	①	②	③	④	⑤	⑥	⑦	⑧
	a_e (mm)	7.70	9.44	9.93	8.28	3.93	1.83	1.08	2.97
	Feed (mm min ⁻¹)	156	127	121	145	300	300	300	300
	MRR (mm ³ s ⁻¹)	59.98	60.02	60.01	59.99	58.95	27.45	16.20	44.55

Table 4 Sample processing conditions for the wave shape (straight cutting)

Constants		Spindle rotation speed = 1,250 rpm, $a_p = 3$ mm							
Conventional	a_e (mm)	5.50							
	Feed (mm min ⁻¹)	150, constant							
	MRR (mm ³ s ⁻¹)	41.25 (average value)							
One-factor control	Section	①	②	③	④	⑤	⑥	⑦	⑧
	a_e (mm)	1.94	1.45	4.07	10.04	11.96	11.55	9.67	5.44
	Feed (mm min ⁻¹)	300	300	295	120	100	104	124	221
	MRR (mm ³ s ⁻¹)	29.10	21.75	60	60	60	60	60	60

cutting conditions for each “curved cutting” and “straight cutting” step. To calculate instantaneous cutting volumes, the path was divided into eight parts (each of 30°) and the average cutting value per section was used. The upper limit of the feed rate was set to 300 mm min⁻¹ as the material included a section with a very low MRR. If machining were more rapid, the machining quality and surface roughness might deteriorate, which is associated with premature tool damage.

2.2.2 Two-factor Control Method

The two-factor control method adjusts both the spindle rotation speed and the feed rate to further optimize the process. Here, the MRR was maximized while maintaining the feed per tooth. As for the one-factor control method, the feed factor is equated to the MRR calculated from the cutting power, $P_{cutting}$; however, the feed per tooth was maintained constant largely to avoid excessive wear of the cutting tool edge. Changes in spindle rotation speed may influence process stability. Thus, the process parameters need to be carefully adjusted by monitoring whether unexpected fluctuations occur in the power profile.

Also, to hold the cutting conditions within reasonable ranges, the maximum MRR and the spindle rotation speed were limited. The MRR was limited to 90 mm³ s⁻¹ for the stepped shape (the same as for the one-factor control method). The upper limit of spindle rotation speed was set to 1,850 rpm. The tool diameter is 12 mm; the spindle rotation speed (N) thus ranges from 795.8–1,856.8 rpm over the recommended cutting speed (V_c) of 30–70 m min⁻¹ (Eq. 1).

$$V_c = \frac{\pi * D * N}{1,000} \quad (1)$$

where V_c = Cutting speed (m min⁻¹). D = Diameter of the endmill. N = Spindle rotation speed (rpm)

Both the stepped and wave shapes were similarly tested. Table 5 shows the experimental conditions for stepped shaping. For the conventional group, the same cutting conditions were adopted defined in the former section. Under such conditions, the calculated feed per tooth was 0.030 mm per flute at a feed rate of 150 mm min⁻¹. In the two-factor control group, the feed rate and the spindle rotation speed were maximized (but neither exceeded its upper bound). The path was divided as for the one-factor control method (above). Tables 6 and 7 show the cutting conditions at each step for the wave shape.

3 Results

3.1 The Comprehensive Power Consumption Model

An empirical power consumption model was constructed based on experimental data and the response surface method (RSM). The model uses terms of up to second-order to predict total power consumption P_{total} under any cutting condition with an accuracy exceeding 92%. The principal effects of each factor on total power consumption are shown in Fig. 5.

All cutting factors correlated positively with the total power consumption. Increases in a_p and a_e exerted the

Table 5 Sample processing conditions of the two-factor control method used to create stepped shapes

Radial depth of cut a_e (mm)		4	8	12	8	4
Constants		Feed per tooth = 0.030 mm flute ⁻¹ $a_p = 3$ mm				
Conventional	Feed (mm min ⁻¹)	150, constant				
	Spindle rotation speed (rpm)	1,250, constant				
	MRR (mm ³ s ⁻¹)	30	60	90	60	30
Two-factor control	Feed (mm min ⁻¹)	222	222	150	222	222
	Spindle rotation speed (rpm)	1,850	1,850	1,250	1,850	1,850
	MRR (mm ³ s ⁻¹)	45	88.33	90	88.33	45

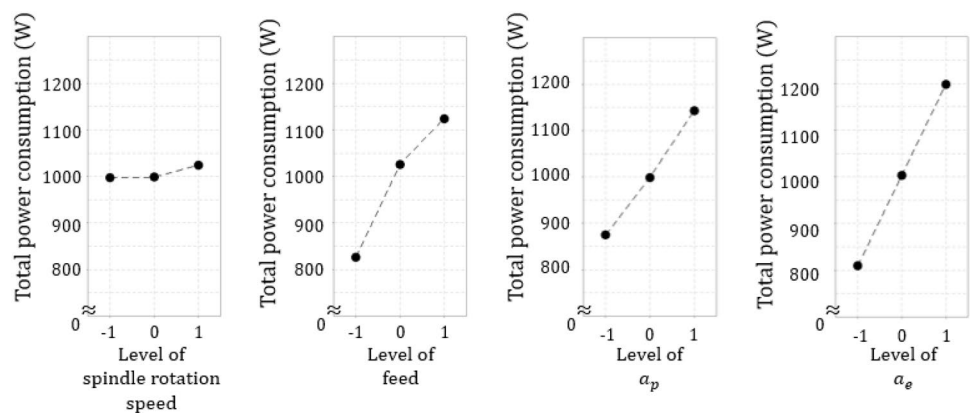
Table 6 The sample processing conditions of the two-factor control method for the wave shape (curved cutting)

Constants		Feed per tooth = 0.030 mm flute ⁻¹ , $a_p = 3$ mm							
Conventional	a_e (mm)	5.30							
	Spindle rotation speed (rpm)	1,250, constant							
	Feed (mm min ⁻¹)	150, constant							
	MRR (mm ³ s ⁻¹)	39.75 (average value)							
Two-factor control	Section	①	②	③	④	⑤	⑥	⑦	⑧
	a_e (mm)	7.70	9.44	9.93	8.28	3.93	1.83	1.08	2.97
	Spindle rotation speed (rpm)	1,850	1,590	1,511	1,811	1,850	1,850	1,850	1,850
	Feed (mm min ⁻¹)	222	191	181	217	222	222	222	222
	MRR (mm ³ s ⁻¹)	85.50	90	90	90	43.66	20.36	11.99	32.95

Table 7 The sample processing conditions of the two-factor control method for the wave shape (straight cutting)

Constants		Feed per tooth = 0.030 mm flute ⁻¹ , $a_p = 3$ mm							
Conventional	a_e (mm)	5.50							
	Spindle rotation speed (rpm)	1,250, constant							
	Feed (mm min ⁻¹)	150, constant							
	MRR (mm ³ s ⁻¹)	41.25 (average value)							
Two-factor control	Section	①	②	③	④	⑤	⑥	⑦	⑧
	a_e (mm)	1.90	1.50	4.10	10	12	11.60	9.70	5.40
	Spindle rotation speed (rpm)	1,850	1,850	1,850	1,500	1,250	1,293	1,546	1,850
	Feed (mm min ⁻¹)	222	222	222	180	150	155	186	222
	MRR (mm ³ s ⁻¹)	21.09	16.65	45.51	90	90	90	90	59.94

Fig. 5 Main effects plots for total power consumption (P_{total})



greatest effects on power consumption, as they are directly related to MRR. The feed effect was greater than that of the spindle rotation speed; a change in spindle rotation speed varied mainly $P_{machine}$, not $P_{cutting}$. As the cutting volume increased, $P_{cutting}$ became greater than $P_{machine}$. Thus, the variation resulting from spindle rotation speed became less significant at higher MRRs.

Three-dimensional surface plots of the average experimental data (circles) are shown in Fig. 6. These reflect the

changes in spindle rotation speed/feed, and a_p/a_e , respectively. Figure 6(a) shows that the feed had a greater effect on power consumption than did the spindle rotation speed. Figure 6, 7, 8b shows that the effect of a_e was greater than that of a_p , because the range of a_p was 2–4 mm whereas that of a_e was 4–12 mm; a_e thus affected total power consumption to a greater extent. However, the total power consumption should be linearly proportional to the absolute MRR. The predictive model includes several interaction

Fig. 6 Surface plots of power consumption vs. spindle rotation speed, feed, a_p , and a_e . **a** Power vs. spindle rotation speed and feed. **b** Power vs a_p and a_e .

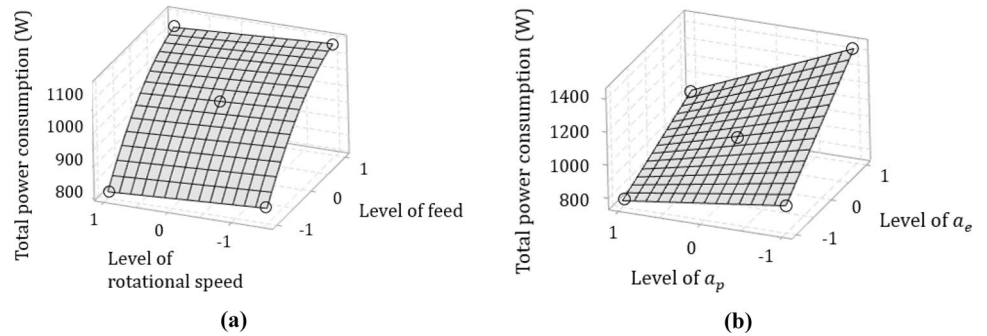


Fig. 7 Power consumption profile for stepped shape machining. **a** Conventional group, **b** One-factor control group

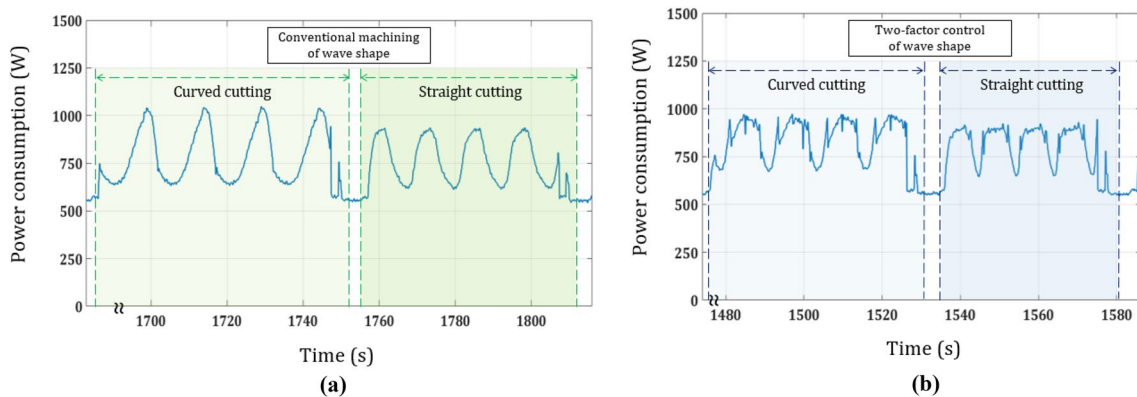
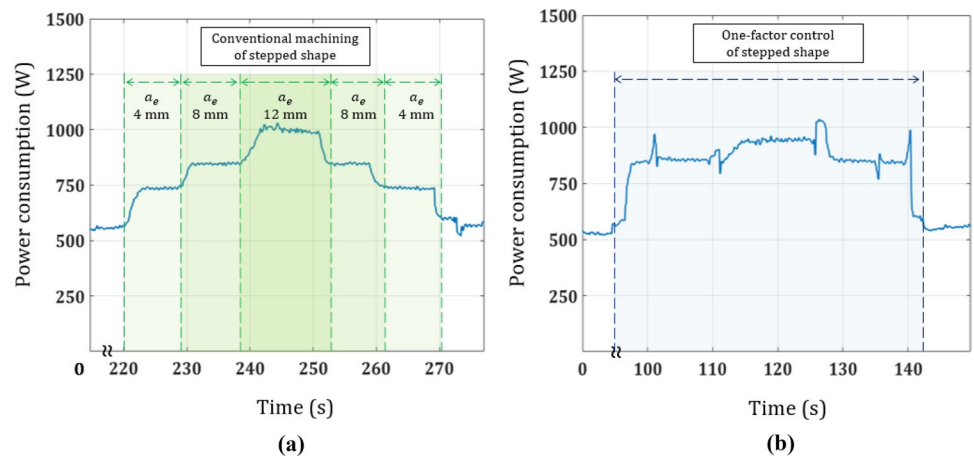


Fig. 8 Power consumption profile for wave shape machining. **a** Conventional group, **b** Two-factor control group

terms but, within certain limits, they can be ignored when designing an AFC strategy.

3.2 The Effects of the Control Methods on Energy and Time

Figures 7 and 8 show examples of power profiles with the suggested control schemes. Figure 7a shows a power profile with the conventional group process parameters for the stepped shape. The power consumption varies mainly in terms of a_e . Figure 7b shows a power profile with the one-factor control process parameters for the stepped shape. By equating a feed to MRR, the power consumption value showed a negligible change compared to Fig. 7a, regardless of the change in cutting volume. The cycle time was also reduced. Figures 8a and b show power profiles with the process parameters in the conventional and two-factor control groups for the wave shape, respectively. Here, four sets of the wave shape were tested. Similar to Fig. 7, the power consumption remains almost the same value regardless of cutting volume change, and the cycle time was reduced.

Table 8 lists the experimental results, and the total energy and cycle-time savings afforded by the two methods when machining different shapes of workpieces. The total energy savings were 6–18% and the cycle time savings 10–26.7%. The predicted results based on the model were accurate; all errors were less than 2%, attributable to delays when changing the cutting conditions. The savings may vary by workpiece geometry, as the schemes afford benefits (savings in energy and time) when machining certain sections but impose costs in other sections. The efficiencies of control schemes, and the differences in energy and time savings, are revisited in more detail in the Discussion.

4 Discussion

To explore how the control schemes save energy in a smart, optimal, and universal manner, the relationships among parameters, and the SECs, were analyzed. The schemes

exploit the fact that the MRR at any moment can be directly monitored by measuring the power consumption. The efficiency of the suggested schemes was then discussed with respect to the changing process parameters as well as the range of parameters. Finally, the effects of mechanical properties of workpieces and the applicability of the scheme were discussed by comparing the results of titanium alloy data to those of other materials.

4.1 From the ‘Smart’ Perspective

Figure 9 shows the experimental results and the data of earlier study [23] using the same cutting tools and machining environment. The earlier study compared the energy consumption of two cutting tools at lower MRR values of less than $50 \text{ mm}^3 \text{ s}^{-1}$, but some of the data were merged into the current study to strengthen the regression curve. The regression line indicates that $P_{machine}$ varies little with the processing conditions, but $P_{cutting}$ generally increases linearly with increasing MRR because the MRR directly reflects the cutting load. The relationship between power consumption and MRR may not appear linearly in too low or too high spindle rotation speed due to the machine’s lubricant viscosity, but

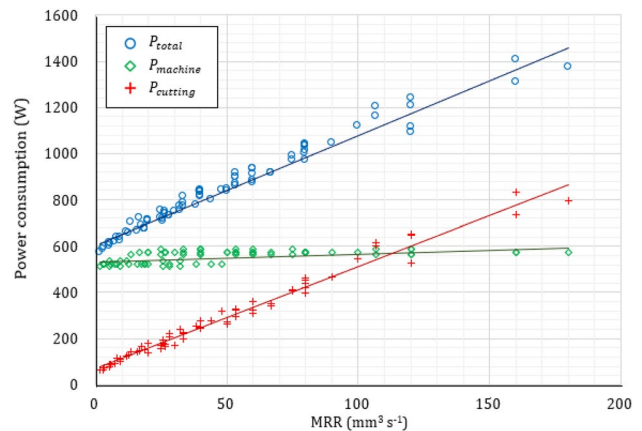


Fig. 9 Power consumption as a function of the MRR

Table 8 The savings afforded by the two methods and the mean error rates

One-factor control (Constant MRR)	Stepped		Wave	
	Total energy (%)	Cycle time (%)	Total energy (%)	Cycle time (%)
Predicted saving	8.00 (4,040 J)	10.00 (6 s)	17.12 (3,710 J)	21.11 (5.88 s)
Measured saving	6.00 (3,030 J)	10.00 (6 s)	15.62 (3,385 J)	22.00 (6.13 s)
Two-factor control (Constant feed per tooth)	Stepped		Wave	
	Total energy (%)	Cycle time (%)	Total energy (%)	Cycle time (%)
Predicted saving	17.09 (9,058 J)	25.95 (15.55 s)	18.32 (3,987 J)	27.09 (7.63 s)
Measured saving	17.07 (9,047 J)	25.98 (15.57 s)	18.10 (3,939 J)	26.71 (7.52 s)

the range of values set in this experiment (1250–1850 rpm) does not correspond to this. At the same MRR, variations in P_{total} are caused by different power consumptions at different spindle rotation speeds. A lower rotation speed is associated with slightly lower power consumption at the same MRR. However, the spindle rotation speed has a negligible effect on the P_{total} (6.54% maximum error at an MRR of $120 \text{ mm}^3 \text{ s}^{-1}$ when P_{total} is $1,241.5 \text{ W}$).

For implementation, the MRR must be identified from the total power consumption in real-time. A power meter is needed, and the process parameters should be read via OPC UA or MTConnect to calculate $P_{machine}$. $P_{cutting}$ is obtained by subtracting $P_{machine}$ (which is not influenced by the material) from P_{total} . Then, the MRR is calculated from the slope of $P_{cutting}$ (Fig. 9). In one-factor control, the feed is adjusted to match the current MRR, or $P_{cutting}$, to the reference value. In two-factor control, the feed factor is similarly adjusted but the spindle rotation speed is also adjusted to maintain the feed per tooth. Figure 10 shows the algorithm to implement the suggested scheme.

Using an external power meter, the process parameters can be adjusted in real-time without any knowledge of the current workpiece geometry or the cutting forces. Given that $P_{cutting}$ is principally dependent on the material (not the machine), the control schemes can be implemented based on an appropriate $P_{cutting}$ reference level (as shown in Figs. 7

and 8), thus without all the information of Fig. 9, but using a literature value or those of a few experimental points. However, $P_{machine}$ and material information are essential. The effect of the reference level on energy-saving is further discussed below.

4.2 From the “Optimal” Perspective

Here, the efficiencies of the control methods as process parameters vary. First, the differences in the saving rates of the two methods are discussed. Second, the effects of the reference levels and the ranges of process parameters on the saving rates are analyzed. The schemes seek to overcome the natural trade-off between increasing MRR (gain) and decreasing MRR (loss) to render our strategy effective. The answers guide the design of a strategy and increase efficiency.

4.2.1 Comparison of the Efficiency of the Two Methods

Figure 11 shows the specific energy consumption (SEC) as a function of the MRR. The SEC (J mm^{-3}) is the energy required to remove a unit volume, thus P_{total} divided by the MRR. In other words, the SEC reflects the relationship between the MRR and energy consumption. As many researchers have shown, the SEC decreases as the MRR

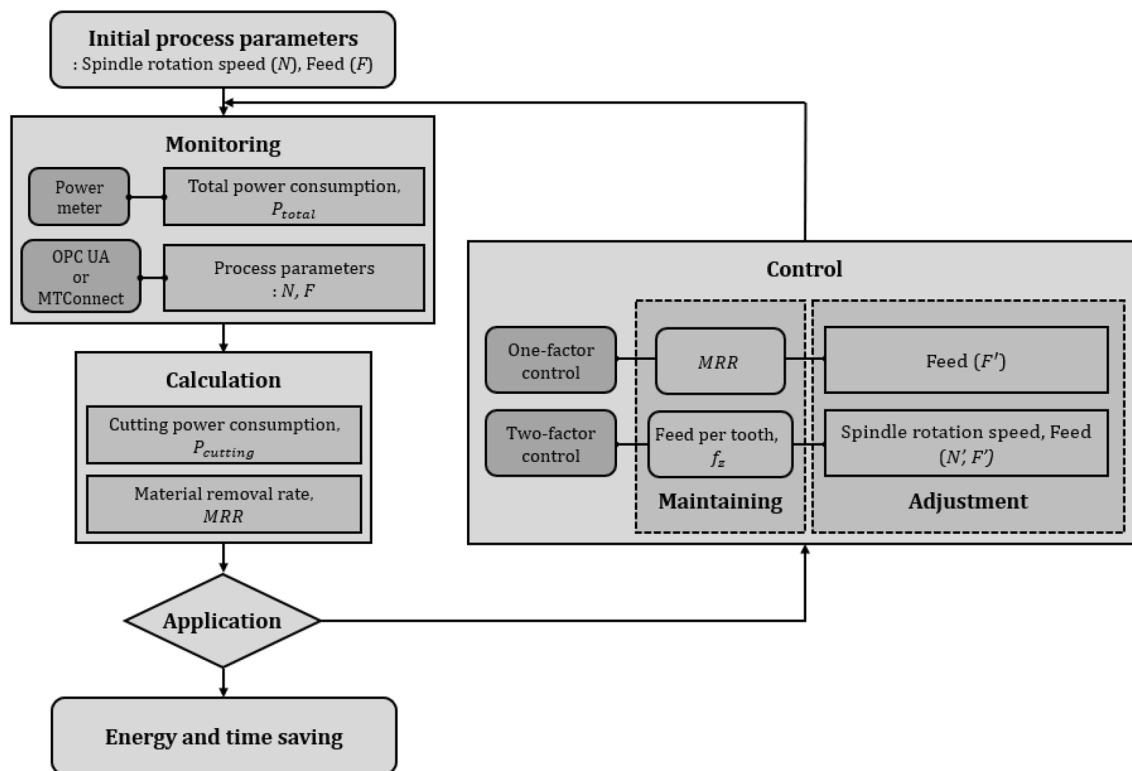


Fig. 10 Algorithm of smart adaptive control

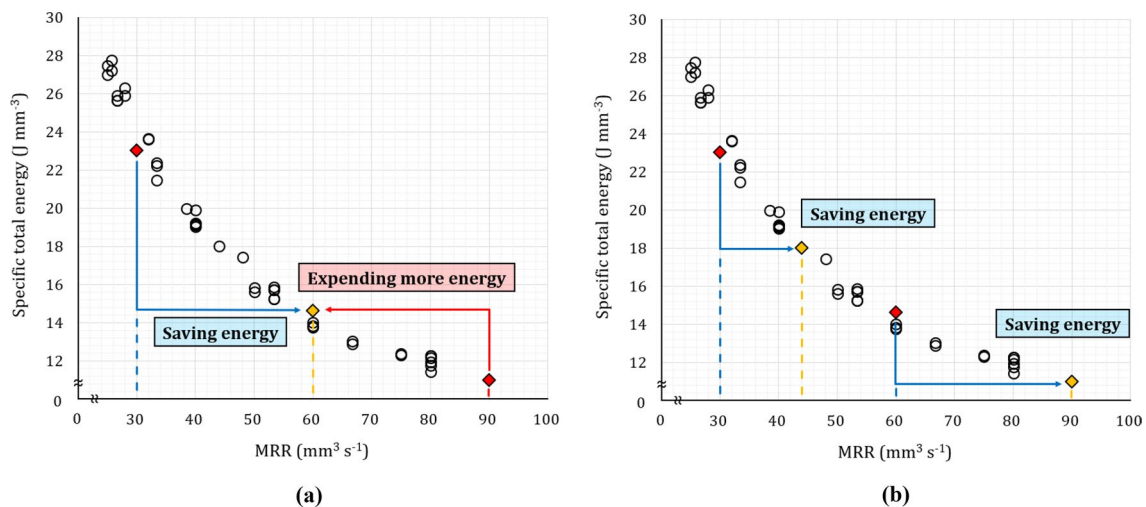


Fig. 11 The specific total energy (STE) vs. MRR diagrams for **a** the one-factor control method and **b** the two-factor control method

increases (as a convergent curve) principally because $P_{machine}$ is fixed. When the MRR increases, the increases in $P_{machine}$ are smaller than those in $P_{cutting}$; thus, P_{total} divided by MRR decreases. Use of the highest possible MRR reduces total energy consumption, but this is generally limited by realistic constraints.

However, the schemes distribute the cutting load (in terms of the MRR) by changing the process parameters. If the current MRR is lower than the reference value, the methods increase the MRR, and vice versa. Hence, the schemes save energy when machining some parts of the workpiece, but consume more energy when machining other parts of the workpiece. Again, the energy-saving may vary by work geometry.

Nevertheless, the schemes are clearly effective in terms of energy saving; they exploit the trade-off between increasing and decreasing MRR. Figure 11a shows the changes in process parameters for the one-factor control method and Fig. 11b those for the two-factor control method. The changes are marked with arrows; the stepped shape serves as an example. In Fig. 11a, the trade-off can be observed. However, given the equal deviations in the MRR from the reference value, the saving is greater than the expenditure because of the shape of the SEC curve. The energy consumption is reduced even with a half-gain-half-loss workpiece. In the two-factor control method (Fig. 11b), the MRR is maximized by increasing the spindle rotation speed, but this speed does not significantly affect the SEC. Thus, the total energy consumption falls.

The difference in the saving rates is explained by the Figures. The one-factor control method distributes the cutting load by maintaining the MRR (constant value of $60 \text{ mm}^3 \text{ s}^{-1}$). For instance, seeing Fig. 11a, increasing MRR from $30 \text{ mm}^3 \text{ s}^{-1}$ to $60 \text{ mm}^3 \text{ s}^{-1}$ could save SEC by about

8.96 J mm^{-3} , while decreasing MRR from $90 \text{ mm}^3 \text{ s}^{-1}$ to $60 \text{ mm}^3 \text{ s}^{-1}$ increased SEC by about 3.09 J mm^{-3} . Thus, the energy consumption is reduced by about 5.87 J mm^{-3} even in a half-gain-half-loss workpiece. On the other hand, the two-factor control method distributes the cutting load by maintaining the feed per tooth with the maximum MRR ($90 \text{ mm}^3 \text{ s}^{-1}$). Hence in the two-factor control, all the changes in process parameters reduce the SEC unlike in the one-factor control and consume less energy for the machining of the same volume despite of higher spindle rotation speed. In Fig. 11b, increasing MRR of the left red dot (with the original MRR of $30 \text{ mm}^3 \text{ s}^{-1}$) could save SEC by about 4.98 J mm^{-3} , and that of the right red dot (with the original MRR of $60 \text{ mm}^3 \text{ s}^{-1}$) could save SEC by about 3.08 J mm^{-3} , respectively. The savings afforded by two-factor control are higher than those of one-factor control.

However, during two-factor control, the SEC reduction decreases if the original (before any change) MRR is high (Fig. 11b). Thus, the efficiency of two-factor control method varies by the MRR in the conventional group; the difference in the saving rates of the two methods falls if the conventional group employs a high MRR. For the wave shape, the two-factor control method afford slightly higher reductions in energy consumption and cycle time compared to the stepped shape, because the MRR (of the conventional group) for the wave shape is lower than that for the stepped shape. In addition to the lower reduction in energy consumption, maintenance of a high spindle rotation speed may reduce tool life.

The choice of an appropriate reference level and range determine the efficiency of a control strategy. If the reference MRR level is too high, no control method saves significant energy, and the risk of tool failure increases. If, however, the MRR is excessively lowered, the fall in machining quality

may become more significant than prevention of tool deterioration. Not only does the cycle time increase but also productivity decreases. The effects of the reference levels and ranges are discussed below.

4.2.2 The Effects of the Reference Level and Constraints

Here, changes in efficiency as the reference levels and ranges vary are discussed. The one-factor control method is dealt with first; this is a relatively simple process with few constraints. Here, the median MRR (the reference level) and the widths of the ranges were varied. The details are shown in Figs. 12–13 and the accompanying savings changes in Tables 9–10. As the median MRR changes, the energy consumption of the conventional group (where no parameter changes) varies. Thus, to compare

the efficiencies (not the absolute amount of savings), the energy consumption of the conventional group was considered as the MRR changed, and compared to that of the one-factor control group.

Figure 12 shows the effects of varying the MRR median values. The lowest and highest MRR limits spanned the same intervals (Table 9). The slope of the SEC tangent decreases more markedly when the median value falls. Thus, the growth rate of SEC-mediated energy-saving increases significantly with a decrease in the median MRR. However, a lower median MRR also increases the amount of energy expended. This is why the differences between the energy-saving and time-saving rates become larger at smaller median MRRs. Less energy is saved (compared to cycle time). The ratio of the energy-saving rate to the time-saving rate decreases as the median MRR decreases, as well as the

Fig. 12 The STE vs. MRR graph when the median values of the ranges vary

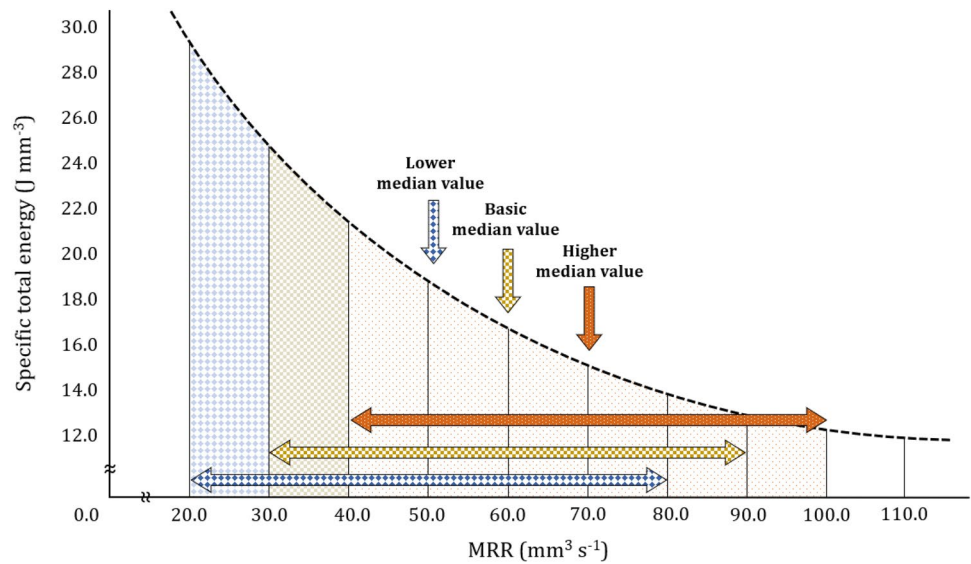


Fig. 13 The STE vs. MRR diagram when the widths of the ranges varied

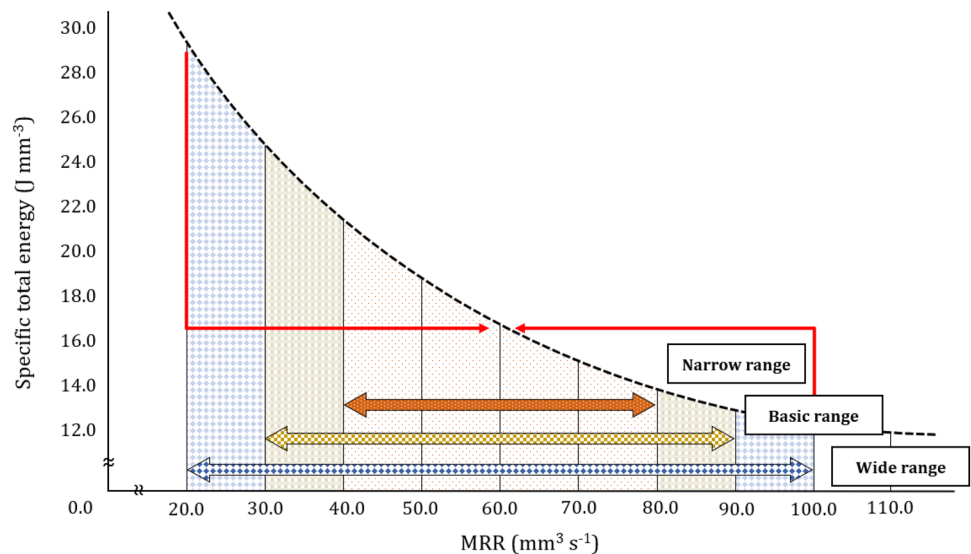


Table 9 The MRR values and the efficiencies when the median values of the ranges varied

	MRR range ($\text{mm}^3 \text{s}^{-1}$)				Energy-saving rate	Time-saving rate
	Median	Lower limit	Center line	Upper limit		
Low	20	50	80		11.7% (6,310 J)	17.2% (12.2 s)
Basic	30	60	90		8.0% (4,040 J)	10.0% (6 s)
High	40	70	100		6.7% (4,363 J)	6.2% (4.56 s)

Table 10 The MRR values and the efficiencies when the limit ranges varied

	MRR range ($\text{mm}^3 \text{s}^{-1}$)				Energy-saving rate	Time-saving rate
	Range	Lower limit	Center line	Upper limit		
Narrow	40	60	80		3.3% (1,666 J)	2.7% (1.62 s)
Basic	30	60	90		8.0% (4,040 J)	10.0% (6 s)
Wide	20	60	100		16.7% (8,433 J)	23.7% (14.22 s)

energy-saving rate itself. Nevertheless, control is effective in terms of both energy- and time-saving at any median MRR.

Figure 13 shows a schematic of the different control ranges. With respect to the work geometry, the control ranges vary from narrow to wide. Although the amount of energy expended increases when the range is wider, energy-saving is more efficient. Thus, use of a wider range better saves both energy and time (Table 10). The ratio of the energy-saving rate to the time-saving rate increases as the control range increases. The control method remains effective in terms of both energy- and time-saving at any median value.

On the other hand, for the two-factor control method, the limit imposed on the maximum spindle rotation speed influences the energy-saving rate; the feed per tooth is maintained. With a higher maximum spindle rotation speed, the process can be performed at higher MRRs. With the same limit, a higher feed per tooth increases the MRR. However, if the MRR is too high, control efficiency decreases, as explained above.

The process could be significantly improved by changing the process parameters of MRRs that are too low. Intuitively, a higher MRR is preferred from the perspective of the total amount of saving. However, Tables 9 and 10 show that the controls are more effective at the lower original MRRs. If the current MRR is adequately high, increasing the MRR will save energy less efficiently and the risks of excessive tool wear or breakage increase. Thus, any change in process parameters should be carefully considered in terms of both effectiveness and efficiency. However, our control methods are effective under all conditions, particularly at lower MRRs.

4.3 From the “Universal” Perspective

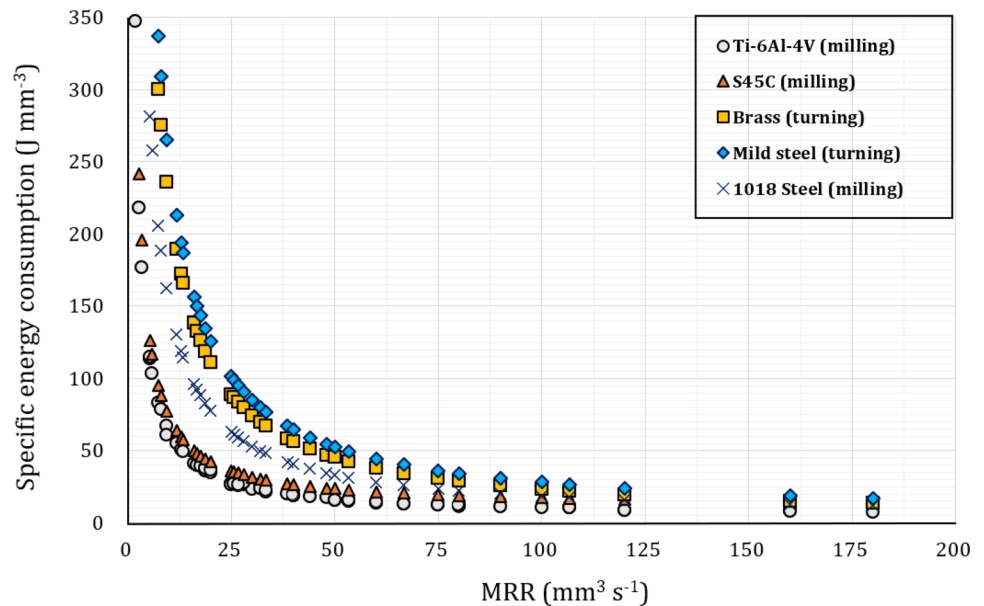
To assess whether our methods are universal, the characteristics of the SECs were discussed via literature review.

In terms of the MRR, a decreasingly convergent curve was commonly observed, because the variation in $P_{machine}$ is smaller than that of $P_{cutting}$. The proportion of $P_{machine}$ in P_{total} varies significantly [26, 27], generally increasing as the machine size increases, rendering our methods more effective. The slope of the SEC curve will be larger, as will the energy and time savings.

Furthermore, milling of titanium alloy was compared to milling of S45C and 1018 steel, and turning of brass and mild-steel. Ti-6Al-4 V exhibits a relatively high yield strength (828 MPa); S45C, 1018 steel, brass, and mild steel have lower yield strengths (S45C 585 MPa, 1018 Steel 370 MPa, brass 255 MPa, mild steel 250 MPa). Figure 14 expresses the SEC values as functions of the MRRs of the materials. The SEC vs. MRR plot of S45C in Fig. 14 was calculated by reference to Li et al. [28] and the 1018 steel data was calculated by reference to Diaz et al. [29] and the brass and mild-steel turning data were calculated based on the work of Kara and Li [30]. The SEC curves for different types of machining and different materials are of similar shape but different magnitudes. Thus, our methods would be effective using any material, in particular at low MRRs. If the slope of the SEC curve is high (for titanium alloy, for example), the energy- and time-saving rates will be high. The machining environment will not change the (decreasing) convergent trend, only the values [31]. Thus, the control methods will be effective when using various tools and cutting fluids, and even during other types of machining, such as turning or drilling.

Further, titanium alloy is a representative difficult-to-cut material because of its low thermal conductivity. [32, 33] Heat generated during machining cannot be rapidly dispersed, reducing productivity. Nevertheless, the energy consumption and cycle time were successfully reduced using the conditions defined here, without significant problems.

Fig. 14 SEC vs. MRR graphs for other types of machining and materials



5 Conclusion

Control schemes were suggested based on measured power consumption; the scheme was discussed from the “*smart, optimal, and universal*” perspectives. MRR calculation based on the power model enables direct and precise changes in parameters without the need to measure a force or the spindle load (“*smart*” perspective). The schemes can be applied without a full power model, thus by employing only an appropriate reference level, which does not have to be very high (“*optimal*” perspective). Furthermore, this method will cope with any material (“*universal*” perspective). The suggested schemes were effective in energy- and time-saving and at least 15% of energy could be saved with the given workpiece. Furthermore, from the SEC curve, it was confirmed that the schemes would be effective even in half-gain-half-loss workpieces. Despite the trade-off relationship, the gain was more than 2 times the loss in the suggested schemes with the given conditions. The effects of the material characteristics were also discussed, as were the effects of the reference levels and control range. The experimental data and discussion offer insights into efficient strategies even when process and material knowledge are limited.

The suggested schemes are under development for implementation in real machine tools. A power meter was connected to a human–machine interface (HMI) and the MRR was calculated via $P_{cutting}$. The process parameters were changed; the feed and spindle rotation varied. Early works proved that the process could be successfully controlled with a delay of less than 0.1 s, without full knowledge of materials or cutting geometries. It is expected that utilization of

the power consumption data can contribute to the development of “*smart, optimal, and universal*” strategies, that can be applied even to the machining of complex shapes. Also, the research to optimize coolant pumping by monitoring the power data is being contrived; adaptive control will be extended to the coolant pump. It is believed that these efforts will facilitate eco-friendly sustainable manufacturing.

Acknowledgements This work was supported by the National Research Foundation of Korea (NRF) grant funded by the Korean government (Ministry of Science and ICT and Ministry of Education) (No. NRF-2022R1F1A1063896 and No. 5199990714521) and by the Korea Evaluation Institute of Industrial Technology (KEIT) grant funded by the Korean government (Ministry of Trade, Industry, and Energy, No. 20003806).

Declarations

Conflict of Interest The authors declare that they have no known competing financial interests or personal relationships that could have appeared to influence the work reported in this paper.

References

- Schlosser, R., Klocke, F., Lung, D. (2011). Sustainability in manufacturing - Energy consumption of cutting processes. *Advances in Sustainable Manufacturing*, 85–89.
- Denkena, B., Abele, E., Brecher, C., Dittrich, M. A., Kara, S., & Mori, M. (2020). Energy efficient machine tools. *CIRP Annals*, 69(2), 646–667.
- Dureja, J. S., Singh, R., Singh, T., Singh, P., Dogra, M., & Bhatti, M. S. (2015). Performance evaluation of coated carbide tool in machining of stainless steel (AISI202) under minimum quantity

- lubrication (MQL). *International Journal of Precision Engineering and Manufacturing-Green Technology*, 2(2), 123–129.
4. Pervaiz, S., Anwar, S., Qureshi, I., & Ahmed, N. (2019). Recent advances in the machining of titanium alloys using minimum quantity lubrication (MQL) based techniques. *International Journal of Precision Engineering and Manufacturing-Green Technology*, 6, 133–145.
 5. Boswell, B., Islam, M. N., Davies, I. J., Ginting, Y. R., & Ong, A. K. (2017). A review identifying the effectiveness of minimum quantity lubrication (MQL) during conventional machining. *The International Journal of Advanced Manufacturing Technology*, 92, 321–340.
 6. Sen, B., Mía, M., Krolczyk, G. M., Mandal, U. K., & Mondal, S. P. (2021). Eco-friendly cutting fluids in minimum quantity lubrication assisted machining: A review on the perception of sustainable manufacturing. *International Journal of Precision Engineering and Manufacturing-Green Technology*, 8, 249–280.
 7. Kadirgama, K. (2021). A comprehensive review on the application of nanofluids in the machining process. *The International Journal of Advanced Manufacturing Technology*, 115, 2669–2681.
 8. Yang, Y., Wang, Y., Liu, Q. (2018). Design of a milling cutter with large length-diameter ratio based on embedded passive damper. *Journal of Vibration and Control*, 25(3).
 9. Sousa Victor, F. C., & Silva Francisco, J. G. (2020). Recent advances on coated milling tool technology-A comprehensive review. *Coatings*, 10(3), 235.
 10. Bermingham, M. J., Palanisamy, S., Morr, D., Andrews, R., & Dargusch, M. S. (2014). Advantages of milling and drilling Ti-6Al-4V components with high-pressure coolant. *The International Journal of Advanced Manufacturing Technology*, 72, 77–88.
 11. Denkena, B., Helmecke, P., & Hulsemeyer, L. (2014). Energy efficient machining with optimized coolant lubrication flow rates. *Procedia CIRP*, 24, 25–31.
 12. Drake, R., Yildirim, M.B., Twomey, J., Whitman, L., Ahmad, J., Lodhia, P. (2006). Data collection framework on energy consumption in manufacturing. *Industrial Engineering Research Conference*. Institute of Industrial Engineers Annual Meeting (May 15–19, Orlando, FL).
 13. Yoon, H. S., Lee, J. Y., Kim, M. S., Kim, E., Shin, Y. J., Kim, S. Y., Min, S., & Ahn, S. H. (2019). Power consumption assessment of machine tool feed drive units. *International Journal of Precision Engineering and Manufacturing-Green Technology*, 7, 455–464.
 14. Yazar, Z., Koch, K. F., Merrick, T., & Altan, T. (1994). Feed rate optimization based on cutting force calculations in 3-axis milling of dies and molds with sculptured surfaces. *International Journal of Machine Tools and Manufacture*, 34(3), 365–377.
 15. Mannan, M. A., Broms, S., & Lindstrom, B. (1989). Monitoring and adaptive control of cutting process by means of motor power and current measurements. *CIRP Annals*, 38(1), 347–350.
 16. Xie, J., Zhao, P., Hu, P., Yin, Y., Zhou, H., Chen, J., & Yang, J. (2021). Multi-objective feed rate optimization of three-axis rough milling based on artificial neural network. *The International Journal of Advanced Manufacturing Technology*, 114, 1323–1339.
 17. Layegh, S.E., Erdim, H., Lazoglu, I. (2012). Offline force control and feedrate scheduling for complex free form surfaces in 5-axis milling. *Procedia CIRP*, 96–101.
 18. Li, Z. Z., Zhang, Z. H., & Zheng, L. (2004). Feedrate optimization for variant milling process based on cutting force prediction. *The International Journal of Advanced Manufacturing Technology*, 24, 541–552.
 19. Ridwan, F., & Xu, X. (2013). Advanced CNC system with in-process feed rate optimization. *Robotics and Computer-Integrated Manufacturing*, 29, 12–20.
 20. Hoang, A. T., Pham, V. V., & Nguyen, X. P. (2021). Integrating renewable sources into energy system for smart city as a sagacious strategy towards clean and sustainable process. *Journal of Cleaner Production*, 305, 127161.
 21. Liang, Q., Zhang, D., Coppola, G., Mao, J., Sun, S., Wang, W., & Ge, Y. (2016). Design and analysis of a sensor system for cutting force measurement in machining processes. *Sensors*, 16(1), 70.
 22. Luan, X., Zhang, S., Li, G. (2018). Modified Power Prediction Model Based on Infinitesimal Cutting Force during Face Milling Process. *International Journal of Precision Engineering and Manufacturing-Green Technology*, 5(1), 71–80.
 23. Lee, J. H., Kim, H. Y., & Yoon, H. S. (2019). Sustainability analysis in titanium alloy machining. *Journal of the Korean Society of Manufacturing Process Engineers*, 18(12), 73–81.
 24. Yoon, H. S., Singh, E., & Min, S. (2018). Empirical power consumption model for rotational axes in machine tools. *Journal of Cleaner Production*, 196, 370–381.
 25. Han, F., Li, L., Cai, W., Li, C., Deng, X., & Sutherland, J. W. (2020). Parameters optimization considering the trade-off between cutting power and MRR based on Linear Decreasing Particle Swarm Algorithm in milling. *Journal of Cleaner Production*, 262, 121388.
 26. Kordonowy, D.N. (2002). A power assessment of machining tools. Thesis (B.S.). *Massachusetts Institute of Technology*. Department of Mechanical Engineering.
 27. Morandnazhad, M., & Unver, H. O. (2017). Energy consumption characteristics of turn-mill machining. *The International Journal of Advanced Manufacturing Technology*, 91, 1991–2016.
 28. Li, L., Yan, J., & Xing, Z. (2013). Energy requirements evaluation of milling machines based on thermal equilibrium and empirical modeling. *Journal of Cleaner Production*, 52(1), 113–121.
 29. Diaz, N., Redelsheimer, E., Dornfeld, D. (2011). Energy consumption characterization and reduction strategies for milling machine tool use. *Globalized Solutions for Sustainability in Manufacturing*, 263–267.
 30. Kara, S., & Li, W. (2011). Unit process energy consumption models for material removal processes. *CIRP Annals*, 60(1), 37–40.
 31. Zhou, L., Li, J., Li, F., Xu, X., Wang, L., Wang, G., & Kong, L. (2017). An improved cutting power model of machine tools in milling process. *International Journal of Advanced Manufacturing Technology*, 91, 2383–2400.
 32. Bagherzadeh, A., Kuram, E., Budak, E. (2021). Experimental evaluation of eco-friendly hybrid cooling method in slot milling of titanium alloy. *Journal of Cleaner Production*, 289(20).
 33. Pramanik, A. (2014). Problems and solutions in machining of titanium alloys. *The International Journal of Advanced Manufacturing Technology*, 70, 919–928.

Publisher's Note Springer Nature remains neutral with regard to jurisdictional claims in published maps and institutional affiliations.

Springer Nature or its licensor holds exclusive rights to this article under a publishing agreement with the author(s) or other rightsholder(s); author self-archiving of the accepted manuscript version of this article is solely governed by the terms of such publishing agreement and applicable law.



Jung-Jae Won majored in Mechanical Engineering in the School of Aerospace and Mechanical Engineering at Korea Aerospace University (KAU). He received B.S. in Aerospace and Mechanical Engineering from Korea Aerospace University in 2021. His research interest is Smart/Hybrid Manufacturing.



Sang Won Kim is currently an associate research engineer at Duckheung Co. Ltd., and a Ph.D. candidate in the Department of Mechanical Hybrid Engineering at Gyeongsang National University. He received his B.S. in 2013, and M.S. in 2021 all in Mechanical System Engineering from Gyeongsang National University. His research interests are Machine Tools and Unattended Automation.



Yong Ju Lee is currently a M.S. candidate in the Department of Smart Air Mobility and School of Aerospace and Mechanical Engineering at Korea Aerospace University (KAU). He received his B.S. in Aerospace and Mechanical Engineering from Korea Aerospace University in 2020. His research interests are Smart/Hybrid Manufacturing and Sustainable Manufacturing.



Hae-Sung Yoon is currently an Associate Professor in the School of Aerospace and Mechanical Engineering at Korea Aerospace University (KAU). He received his B.S. in 2010, and Ph.D. in 2015 (M.S. integrated) all in Mechanical and Aerospace Engineering from Seoul National University, Korea. Since then, he has held professional positions as a Post-doctoral Fellow in BK21+ Program at Seoul National University from 2015 to 2016, and as a Research Associate in the



Yu-Jin Hur majored in Mechanical Engineering in the School of Aerospace and Mechanical Engineering at Korea Aerospace University (KAU). She received B.S. in Aerospace and Mechanical Engineering from Korea Aerospace University in 2021. Her research interest is Sustainable Manufacturing.

Department of Mechanical Engineering at the University of Wisconsin-Madison, USA, from 2016 to 2018. Yoon's research interests are in Hybrid/Smart Manufacturing, Sustainable Manufacturing, Ultra-precision Machining, Micro/Nano Fabrication, 3D/4D Printing, Manufacturing for Design, and Smart Materials.